

# Half-Mode SIW BPF Loaded with S-Shaped Complementary Spiral Resonators

Feng Wei<sup>1</sup>, Hao Jie Yue<sup>1, \*</sup>, Jing Pan Song<sup>1</sup>, Hong Yi Kang<sup>1</sup>, and Bin Li<sup>2</sup>

**Abstract**—A compact wideband bandpass filter (BPF) based on half-mode substrate integrated waveguide (HMSIW) is proposed in this paper. The proposed BPF is achieved by etching a couple of S-shaped complementary spiral resonators (S-CSRs) on the top layer of HMSIW cavity to achieve a wide passband as well as generate two transmission zeros in the vicinity of the passband respectively to improve the selectivity. In addition, compared with a conventional CSRs-loaded HMSIW structure, the proposed S-CSRs-loaded HMSIW makes the overall size of the filter largely reduced with the same electrical length. Among the HMSIW structures ever reported, the proposed S-CSRs are the first time to be introduced into HMSIW. To validate its practicability, a compact wideband HMSIW BPF loaded with S-CSRs has been designed and implemented through the PCB process. The measured and simulated  $S$ -parameters of the filter are presented to show the proposed filter's predicted performance, and good agreements is obtained between them. This result demonstrates that the newly proposed HMSIW structure loaded with S-CSRs is an excellent candidate for compact filters.

## 1. INTRODUCTION

With the rapid development of miniaturized and high performance devices in modern wireless communication systems, substrate integrated waveguide (SIW) and half mode substrate integrated waveguide (HMSIW) have emerged as attractive alternatives to implement microwave filters due to their excellent advantages of low loss, high  $Q$ -factor, small size and ease of integration with other circuits [1–3]. In order to further reduce the sizes of HMSIW devices, complementary split-ring resonators (CSRRs) and complementary spiral resonators (CSRs) are introduced to design HMSIW bandpass filters (BPFs). By etching the opening resonant ring and its deformation structure on the surface of HMSIW, an evanescent-mode BPF can be realized for producing a passband below the cutoff frequency of the HMSIW. Therefore, the filters designed by this technique can be considered as evanescent-mode filters, resulting in a significant size reduction [4–6]. A CSRRs-loaded SIW filter was presented in [7], which has a larger size and poorer frequency selectivity. An HMSIW BPF loaded with horizontal asymmetrical stepped-impedance CSRRs was proposed in [8]. However, the designed filter has no transmission zero (TZ) below the passband, and the bandwidth is relatively narrow. [9] proposed a 4th order S-band cross-coupled HMSIW filter with wider bandwidth and two TZs in the upper band. However, its effective size is rather large and no TZ at low frequency.

The purpose of the letter is to propose a new approach to design wideband BPFs based on the HMSIW structure for micro- and millimeter-wave applications. In this work, a couple of novel S-shaped complementary spiral resonators (S-CSRs) loaded HMSIW are proposed to operate as resonant unit cells, which work at lower frequency compared with conventional CSRs while occupy the same physical

---

Received 26 March 2018, Accepted 28 May 2018, Scheduled 12 June 2018

\* Corresponding author: Hao Jie Yue (xd\_yhj@163.com).

<sup>1</sup> Collaborative Innovation Center of Information Sensing and Understanding at Xidian University and Science and Technology on Antenna and Microwave Laboratory, Xidian University, Xi'an 710071, P. R. China. <sup>2</sup> School of Information and Electronics, Beijing Institute of Technology, Beijing, P. R. China.

dimensions. Moreover, the proposed S-CSRs can generate a TZ below the passband and broaden the bandwidth of the filter. The parameters of the proposed BPF are simulated to achieve the desired frequency response using the simulator High Frequency Structure Simulator (HFSS), and its electrical equivalent circuit is simulated in Advanced Design System (ADS), which are in good agreement.

## 2. ANALYSIS OF CSR, CSRR AND S-CSR

The layouts of conventional CSR and CSRR are shown in Figures 1(a) and 1(b), respectively. The proposed S-CSR, as given in Figure 1(c), consists of a pair of CSRs connected by a slot. It can be seen that S-CSR has a longer slot length than conventional CSR and CSRR. Therefore, a high level of miniaturization can be achieved by employing S-CSR into HMSIW. In order to validate its practicability, a comparison among the three resonators with the same size is achieved by EM simulation software HFSS 13.0, as shown in Figure 2. The simulated results show that the resonance frequencies of CSRR and CSR are 3.8 GHz and 3.3 GHz, respectively, while S-CSR resonates at much lower frequency (2.8 GHz).

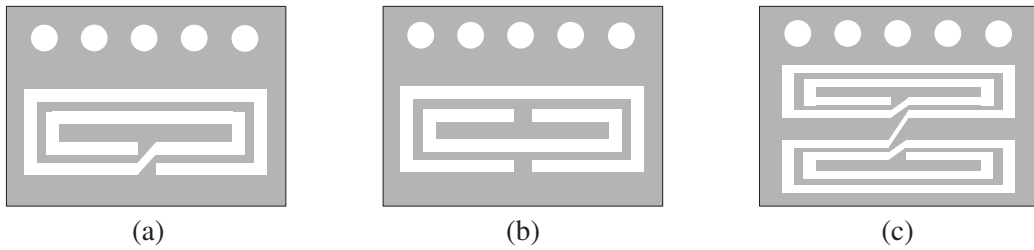


**Figure 1.** Configurations of (a) conventional CSR, (b) conventional CSRR and (c) the proposed S-CSR.

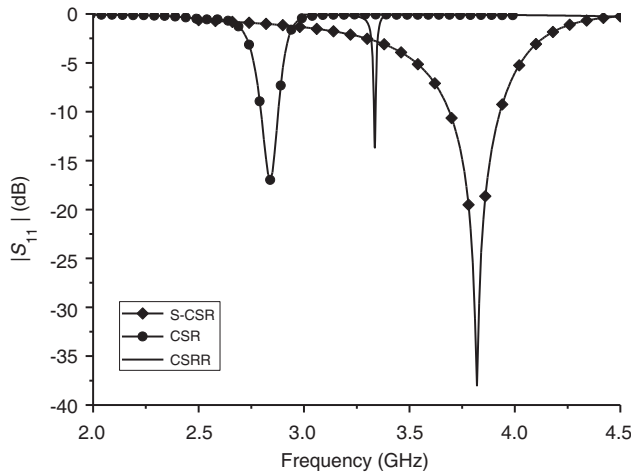


**Figure 2.** Simulated  $|S_{11}|$  parameters of CSR, CSRR and S-CSR with the same size.

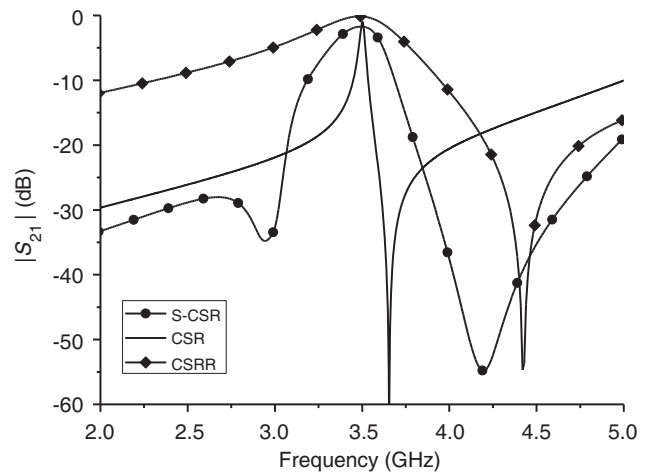


**Figure 3.** Simulated  $|S_{21}|$  parameters of CSR, CSRR and S-CSR with the same resonant frequency.

Moreover, the simulated  $|S_{21}|$  parameters of different HMSIW loaded with CSR, CSRR and S-CSR, respectively, are presented in Figure 3. Compared with HMSIW-CSR and HMSIW-CSRR, it can be seen that the HMSIW BPF loaded with S-CSR can generate a new transmission zero at the low frequency of the passband, which can improve the selectivity of the filter effectively.

### 3. DESIGN OF THE PROPOSED FILTER

An S-CSR unit cell behaves as negative permittivity, and it can provide a stopband when it resonates above the cutoff frequency of the HMSIW. Therefore, a BPF can be obtained by combining the high-pass characteristic of HMSIW with the band-stop characteristic of S-CSR. In order to further broaden the bandwidth and enhance the selectivity of the filter, a pair of S-CSRs loaded coplanar waveguide (CPW) are cascaded into HMSIW, as shown in Figure 4. The electric fields of the CPW's slots on HMSIW are contra-directional. An S-CSR can be excited by the CPW fields at its fundamental resonance frequency for its twisted layout [10]. Meanwhile, the symmetric equivalent circuit model of the proposed HMSIW BPF loaded with S-CSRs is shown in Figure 5(a). The resonant tank formed by  $L_l$  and  $C_r$  models S-CSRs, while  $L_r$  and  $C$  are the equivalent inductance and capacitance of the CPW with the presence of S-CSRs, respectively.  $C_l$  models the line's capacitive gaps, and  $C_c$  models the capacitive coupling of HMSIW with S-CSRs. Moreover,  $L_c$  and  $C_e$  model the inductive and capacitive contributions of HMSIW, respectively. Meanwhile,  $L_e$  models the inductive effect of the via wall. In order to validate its practicability, the circuit simulation is achieved by simulation software Advanced Design System (ADS) 2011. The  $S$ -parameters comparisons between the electromagnetic and circuit simulation are shown in Figure 5(b). It can be seen that a good agreement is obtained. The optimum values are found to be  $L_e = 5.795$  nH,  $C_r = 12.169$  pF,  $C_e = 0.412$  pF,  $L_c = 2.275$  nH,  $C_c = 2.885$  pF,  $L_r = 10.9$  nH,  $C_l = 2.22$  pF,  $L_l = 0.33$  nH,  $C = 4.225$  pF. With the variation of the coupling distance  $g_2$ , the inductance  $L_e$  will be changed accordingly.

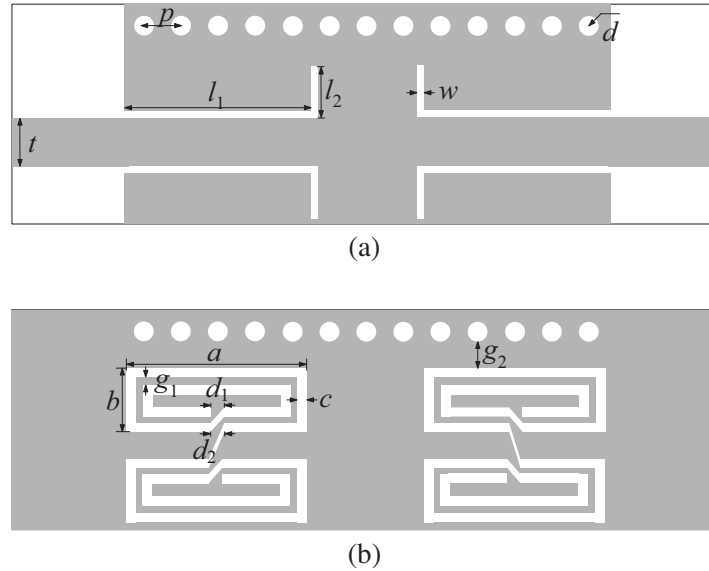


**Figure 4.** Geometry of the proposed wideband HMSIW BPF. (a) Top view and (b) bottom view.

Therefore, the bandwidth of the proposed BPF can be tuned by controlling  $g_2$ . It can be seen from Figure 6(a) that the operating bandwidth of the filter can be adjusted from 400 MHz to 600 MHz when  $g_2$  varies from 0.6 mm to 1.6 mm. Moreover, by changing the length  $b$ , the center frequency of the proposed BPF can be changed, as shown in Figure 6(b). The substrate is F4BM-2 ( $\epsilon_r = 2.2$ ,  $h = 0.8$  mm). All the geometrical parameters are:  $p = 1.45$  mm,  $d = 0.8$  mm,  $t = 2.5$  mm,  $l_1 = 6.85$  mm,  $l_2 = 2.25$  mm,  $w = 0.15$  mm,  $a = 6$  mm,  $b = 2.9$  mm,  $g_1 = 0.4$  mm,  $g_2 = 1.6$  mm,  $d_1 = 0.5$  mm,  $d_2 = 0.5$  mm,  $c = 0.4$  mm.

### 4. SIMULATION AND MEASUREMENT RESULTS

In order to verify the design method, the proposed HMSIW filter is fabricated and measured by using an Agilent network analyzer N5230A. The simulated and measured frequency responses of  $S$ -parameters

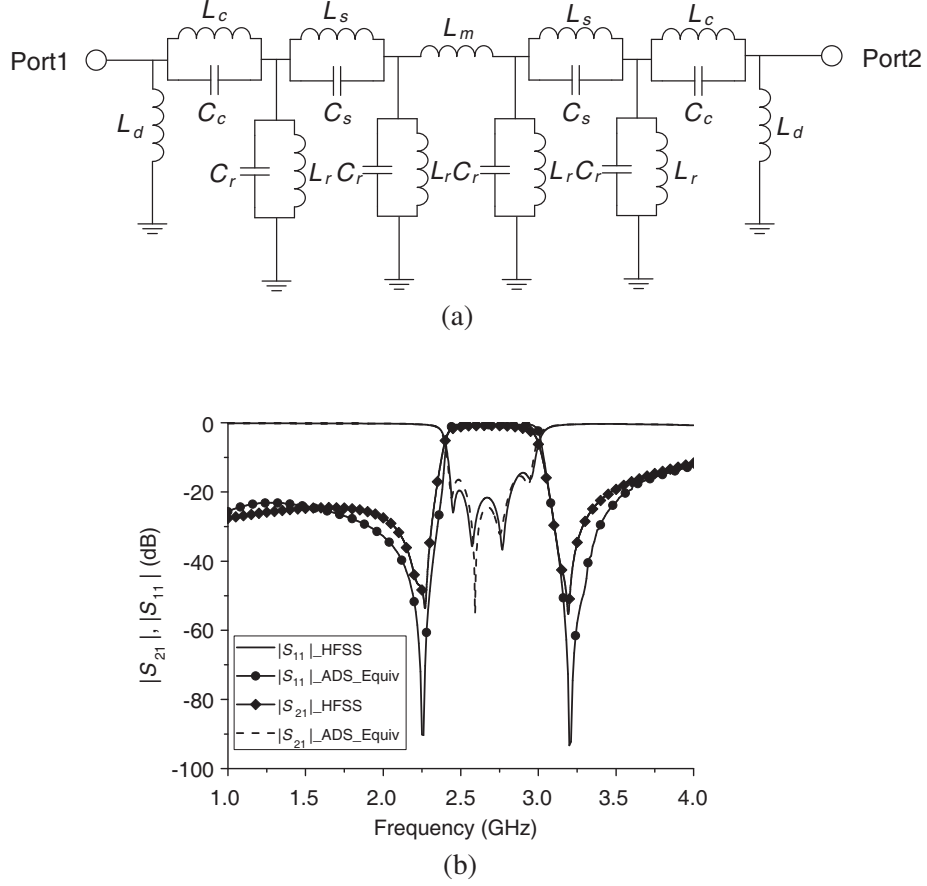


**Figure 5.** (a) Equivalent circuit and (b) performance comparison of the proposed HMSIW BPF loaded with S-CSRs.

of the fabricated filter are shown in Figure 7. The effective dimensions of the fabricated filter are only  $20 \text{ mm} \times 9 \text{ mm}$  ( $0.25\lambda_g \times 0.11\lambda_g$ , where  $\lambda_g$  is the guide wavelength at 2.7 GHz). It can be seen that a fractional bandwidth (FBW) of 22% with the passband ranging from 2.4 to 3.0 GHz is obtained. The max measured insert loss (IL) is less than 1.2 dB, and the return loss is more than 15.0 dB within the passband. In addition, the S-CSRs structure produces two transmission zeros in the lower and upper stop-bands, respectively, which greatly improves the out-of-band selectivity.

The deviations of the measurements from the simulations are expected due to the reflections from the SMA connectors and the finite substrate. Comparisons with the other reported SIW/HMSIW BPFs loaded with resonator cells are listed in Table 1, which further shows that the proposed wideband filter has good performances and realizes miniaturization.

**Table 1.** Comparison with recently published SIW/HMSIW BPFs.

	Effective size ( $\lambda_g$ )	IL (dB)	3 dB FBW (%)	TZs at low frequency
[4]	$0.41 \times 0.18$	1.5	17	No
[6]	$0.67 \times 0.11$	1.1	11.8	No
[7]-IV-A	$0.63 \times 0.31$	2.03	6	No
[8]	$0.29 \times 0.15$	1.53	7.9	No
[9]	$1.27 \times 1.59$	1.25	28	No
Our work	$0.25 \times 0.11$	1.2	22	Yes

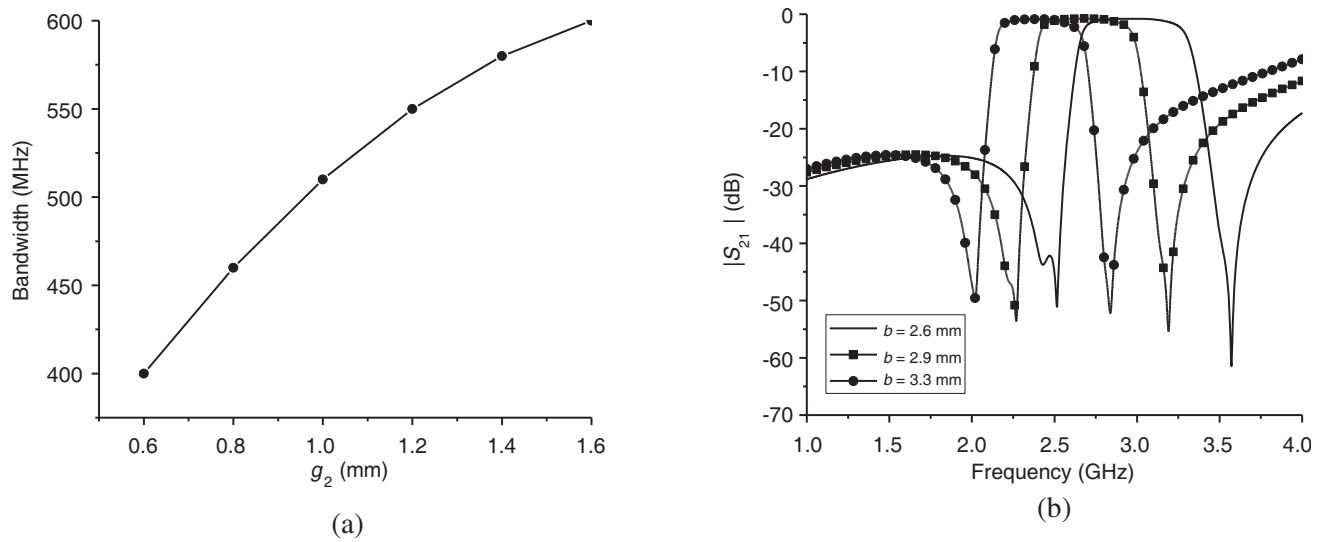


**Figure 6.** (a) Variations of bandwidth with  $g_2$  and (b) variations of frequency with  $b$ .

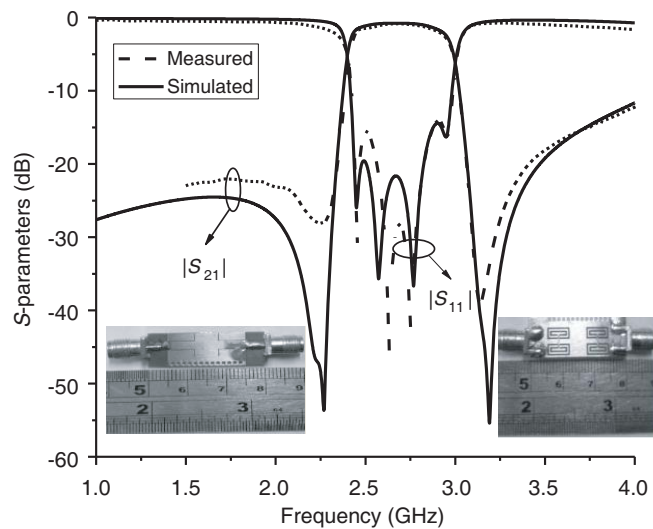


**Figure 7.** Comparison of the simulated and measured results.

### 5. CONCLUSION

In this paper, a novel wideband HMSIW BPF loaded with the proposed S-CSRs is presented, and the feasibility of this design is verified by experimental data of measurement. The size reduction and good frequency selectivity can be achieved by employing a couple of S-CSRs on the top layer of the HMSIW structure. Compared with some reported related works, the proposed filter shows a significant improvement in terms of compact size, broad bandwidth and good selectivity. Good agreements between the simulated and measured results demonstrate the validity of the design. They are also easy to fabricate and integrate with other electric circuits, giving great potential for use in size-reduction microwave circuits.

## ACKNOWLEDGMENT

This work was supported by the National Natural Science Foundation of China (NSFC) (grant 61771055), the Key Laboratory for Research of Design and Electromagnetic Compatibility of High Speed Electronic Systems, Ministry of Education, Basic Research Foundation of Beijing Institute of Technology (grant 20170542009) and the Fundamental Research Funds for the Central Universities (grant JB180204).

## REFERENCES

1. Senior, D. E., A. Rahimi, P. Jao, and Y. K. Yoon, "A surface micromachined broadband millimeter-wave filter using quarter-mode substrate integrated waveguide loaded with complementary split ring resonator," *IEEE MTT-S International Microwave Symposium (IMS 2014)*, 1–4, 2014.
2. Deslandes, D. and K. Wu, "Single-substrate integration technique for planar circuits and waveguide filters," *IEEE Trans. Microw. Theory Tech.*, Vol. 51, 593–596, 2003.
3. Zhang, Q.-L., W. Yin, S. He, et al., "Compact substrate integrated waveguide (SIW) bandpass filter with complementary split-ring resonators (CSRrs)," *IEEE Microw. Wireless Compon. Lett.*, Vol. 20, 426–428, 2010.
4. Chen, X.-P. and K. Wu, "Substrate integrated waveguide cross-coupled filter with negative coupling structure," *IEEE Trans. Microw. Theory Tech.*, Vol. 56, 142–149, 2008.
5. Huang, L. W. and H. Cha, "Novel half-mode substrate integrated waveguide filters with modified broadside-coupled split ring resonators," *IEEE 16th International Conference on Communication Technology (ICCT)*, 548–552, 2015.
6. Cross, L. W., M. J. Almalkawi, and V. K. Devabhaktuni, "Half mode substrate-integrated waveguide-loaded evanescent-mode bandpass filter," *International Journal of Rf & Microwave Computer-aided Engineering*, Vol. 23, No. 2, 172–177, 2013.
7. Dong, Y. D., T. Yang, and T. Itoh, "Substrate integrated waveguide loaded by complementary split-ring resonators and its applications to miniaturized waveguide filters," *IEEE Trans. Microw. Theory Tech.*, Vol. 57, 2211–2223, 2009.
8. Huang, Y. M., Z. H. Shao, W. Jiang, T. Huang, and G. A. Wang, "Half-mode substrate integrated waveguide bandpass filter loaded with horizontal-asymmetrical stepped-impedance complementary split-ring resonators," *Electron. Lett.*, Vol. 52, 1034–1036, 2016.
9. Camdoo, R., S. M. Lau, and H. T. Su, "Compact cross-coupled half-mode substrate integrated waveguide bandpass filter," *IEEE Asia Pacific Microwave Conference*, 706–709, IEEE, 2017.
10. Horestani, A. K., M. Durán-Sindreu, J. Naqui, C. Fumeaux, and F. Martín, "Coplanar waveguides loaded with S-shaped split-ring resonators: Modeling and application to compact microwave filters," *IEEE Antennas Wireless Propag. Lett.*, Vol. 13, 1349–1352, 2014.